Supporting Information

for

A Two-Dimensional Spin-Crossover Coordination Polymer Exhibiting Interlayer Multiple C−H$^{\delta+}$···H$^{\delta-}$−B Dihydrogen Bonds

Jin-Peng Xue, Wen-Jie Wu, Quan-Song Li, Zi-Shuo Yao,* and Jun Tao*

Key Laboratory of Cluster Science of Ministry of Education, School of Chemistry and Chemical Engineering, Liangxiang Campus, Beijing Institute of Technology, Beijing 102488, People's Republic of China.

*E-mail: taojun@bit.edu.cn; zishuoyao@bit.edu.cn

Table of Contents

1. Materials and Methods

Iron(II) chloride tetrahydrate and sodium cyanoborohydride were purchased from Alfa Aesar and Aladdin, respectively. 1,1,2,2-tetrakis(4-(pyridin-4-yl)phenyl)ethane (tppe) was obtained from TCI Shanghai (China). Perchloroethylene was purchased from Aladdin and the other solvents were purchased from Beijing Tong Guang Fine Chemicals Company (China). All reagents were used without further purification.

Variable- and room-temperature powder X-ray diffraction data were recorded on a PANalytical diffractometer with Cu *Kα* radiation equipped with a TTK450 accessory in the temperature range from 123 K to 473 K at an interval of 25 K.

Magnetic measurements were performed on Quantum Design MPMS XL7 magnetometer working in the 2–400 K temperature range with 1 K min^{-1} sweeping rate under a magnetic field of 5000 Oe.

Infrared spectra (KBr pellets) were conducted in the range of 400–4000 cm^{-1} on a Thermo IS5 spectrometer. Elemental analyses for C, H, and N were performed on a EUROVECTER EA3000 analyzer.

Differential scanning calorimetry (DSC) measurements were recorded in an aluminium closed pan on PerkinElmer DSC 8000.

Thermogravimetric (TG) analyses were carried out under nitrogen atmosphere on a TG-DTA 6200 instrument with a heating rate of 10 °C min^{-1}.

Single-crystal X-ray diffraction data were recorded on a Rigaku Oxford XtaLAB PRO diffractometer with graphite-monochromated Mo *Kα* radiation (λ = 0.71073 Å) at 293 and 123 K, respectively. The structure was solved by direct methods and further refined by full-matrix least-squares techniques on F^2 with SHELXL-97.[1] Non-hydrogen atoms were refined anisotropically, and the hydrogen atoms were generated geometrically and refined isotropically. Attempts to define the highly disordered solvent molecules were unsuccessful, so the structure was refined with the PLATON[2] "SQUEEZE" procedure. Void channels were calculated by Mercury[3] "Void" command. CCDC numbers: **1·5C_2Cl_4·4CH_3OH** at 123 K, 1957151; **1·5C_2Cl_4·4CH_3OH** at 293 K, 1957152; **1·3$CHCl_3$·4CH_3OH** at 150 K, 1957153; **1·2C_6H_6·4CH_3OH** at 295 K, 1957154.

2. Synthesis

Synthesis of 1·5C_2Cl_4·4CH_3OH: A 4 mL tetrachloroethylene (TCE)/CH_3OH solution (v/v = 3:1) of tppe (12.8 mg, 0.02 mmol) was placed in one side of an H-type tube, and a CH_3OH solution (5 mL) of [$Fe(NCBH_3)_2$] (0.05 mmol in 5 ml) was placed in another side of the H-type tube. Then, methanol was

carefully added to the top of the two solutions until the H-type tube was entirely filled. After 3 weeks, bright yellow crystals suitable for X-ray diffraction analysis were obtained. The amount of solvent molecules in the crystal was estimated by elemental and thermogravimetric analyses. FTIR (KBr pellet, cm^{-1}): 738, 758, 817, 1006, 1115, 1223, 1400, 1491, 1539, 1607, 2181, 2340, 3031. Elemental analysis calcd (%) for $C_{62}H_{54}O_4N_6B_2Cl_{20}Fe$: C 42.96, H 3.14, N 4.85; found: C 43.01, H 3.04, N 4.84. Elemental analysis calcd (%) for the solvent-free sample (under vacuum at 80 °C for 8 h, $C_{48}H_{38}N_6B_2Fe$): C 74.26, H 4.93, N 10.83. Found C 74.14, H 4.87, N 10.81. IR (KBr pellet, cm^{-1}): 668, 738, 758, 817, 1006, 1068, 1114, 1223, 1401, 1490, 1534, 1608, 2179, 2358, 3030.

Synthesis of 1·3CHCl$_3$·4CH$_3$OH: A 4 mL $CHCl_3$/CH_3OH solution (v/v = 1:1) of tppe (12.8 mg, 0.02 mmol) was placed in one side of an H-type tube, and a CH_3OH solution (5 mL) of $[Fe(NCBH_3)_2]$ (0.05 mmol in 5 ml) was placed in another side of the H-type tube. Then, methanol was carefully added to the top of the two solutions until the H-type tube was entirely filled. After 3 weeks, bright yellow crystals suitable for X-ray diffraction analysis were obtained. The amount of solvent molecules in the crystal was estimated by elemental and thermogravimetric analyses. FTIR (KBr pellets, cm^{-1}): 507, 738, 758, 816, 1006, 1068, 1113, 1222, 1399, 1489, 1539, 1607, 2179, 2331, 3029. Elemental analysis calcd (%) for $C_{55}H_{57}O_4N_6B_2Cl_9Fe$: C 52.40, H 4.40, N 6.67; found: C 52.34, H 4.55, N 6.60.

Synthesis of 1·2C$_6$H$_6$·4CH$_3$OH: A 4 mL C_6H_6/CH_3OH solution (v/v = 1:3) of tppe (12.8 mg, 0.02 mmol) was placed in one side of an H-type tube, and a CH_3OH solution (5 mL) of $[Fe(NCBH_3)_2]$ (0.05 mmol in 5 ml) was placed in another side of the H-type tube. Then, methanol was carefully added to the top of the two solutions until the H-type tube was entirely filled. After 3 weeks, bright yellow crystals suitable for X-ray diffraction analysis were obtained. The amount of solvent molecules in the crystal was estimated by elemental and thermogravimetric analyses. FTIR (KBr pellets, cm^{-1}): 738, 758, 817, 1006, 1115, 1223, 1400, 1490, 1539, 1607, 2181, 2340, 3031. Elemental analysis calcd (%) for $C_{64}H_{66}O_4N_6B_2Fe$: C 72.61, H 6.09, N 7.94; found: C 72.70, H 6.13, N 7.71.

Guest Exchange: Solvent exchanges were performed by immersion of the as-synthesized sample **1**·2C_6H_6·4CH_3OH (~ 20 mg) in various ratios of CH_3OH-C_2Cl_4 mixed solvent (20 mL; 10:0, 9:1, 8:2, 7:3, 6:4, 5:5, 4:6, 3:7, 2:8, 1:9, 0:10) for 6 hours, and each exchange was successively conducted in freshly prepared CH_3OH-C_2Cl_4 mixed solvent for 5 times.

3. Computational Details

The geometries of the monomers and complex were fully optimized at the density functional theory–B3LYP method[4] with 6-31+g(d,p) basis set. Vibrational frequency analysis was performed at the same theoretical level to ensure that the optimized geometries were local minima on their potential energy surfaces. The counterpoise technique proposed by Boys and Bernardi[5] was used to rectify the

interaction-energy calculation (ΔE), geometry optimizations, and frequency computations. All calculations were performed with the Gaussian 09 program package.[6]

4. Standardization of the C−H and B−H bond lengths:

The C_6H_6…$NCBH_3^-$ portion with normalised C–H (1.09 Å) and B–H (1.21 Å) bonds were modelled with AutoCAD software. The coordinates of the hydrogen atom were obtained by the model and hydrogen atoms were generated by Material studios.

5. Additional Tables

Table S1. Crystal data and structural refinements for **1**·$5C_2Cl_4$·$4CH_3OH$

	1·$5C_2Cl_4$·$4CH_3OH$	
T / K	293	123
Formula	$C_{64}H_{58}B_2N_6O_4Cl_{20}Fe$	
M_r / g mol^{-1}	1723.75	
Space group	*Immm*	*Immm*
Crystal system	Orthorhombic	Orthorhombic
a / Å	14.6833(8)	14.6181(7)
b / Å	17.0045(8)	17.3106(15)
c / Å	17.9179(14)	16.5365(8)
α / deg	90	90
β / deg	90	90
γ / deg	90	90
V / Å^3	4473.8(5)	4184.5(5)
Z	16	16
D_c / g cm^{-3} (solvent-free)	0.576	0.616
μ / mm^{-1}	0.188	0.201
F(000)	808.0	808.0
$R1$ [$I \geq 2\sigma(I)$]	0.0702	0.0903
$wR2$ [all data]	0.2307	0.2878

Table S2. The experimental values for selected distances and angles of C−H$^{\delta+}$···H$^{\delta-}$−B DHBs interactions of **1**·5C_2Cl_4·4CH_3OH at 123 K.

entry	C−H···H−B	H···H (Å)	C−H···H (º)	H···H−B (º)
1	C#1 10−H#1 10···H#1 1C−B#1 1	2.5811	122.228	98.788
2	C#1 10−H#1 10···H#1 1A−B#1 1	2.4735	162.539	104.488
3	C#1 10−H#1 10···H#1 1A−B#1 1	2.3100	140.151	137.956
4	C#3 9−H#3 9···H#1 1A−B#1 1	2.4709	115.465	124.443
5	C#4 10−H#4 10···H#1 1B−B#1 1	1.9847	145.951	139.962
6	C#1 9−H#1 9···H#2 1C−B#2 1	2.2429	136.997	145.205
7	C#3 10−H#3 10···H#2 1A−B#2 1	2.0175	140.298	136.570
8	C#2 10−H#2 10···H#2 1C−B#2 1	2.7332	120.949	91.263
9	C#2 10−H#2 10···H#2 1B−B#2 1	2.3329	163.572	112.646
10	C#4 9−H#4 9···H#2 1B−B#2 1	2.6078	112.220	115.204

Table S3. Selected bond lengths and angles for **1**·5C_2Cl_4·4CH_3OH at 293 K**.**

Fe1–N1	2.126(5)
Fe1–N2	2.215(3)
N1–Fe1–N2	90.0
N1–Fe1–N1$^{\#1}$	180.0
N1–Fe1–N2$^{\#1}$	90.0
N1–Fe1–N2$^{\#2}$	90.0

N1–Fe1–N2$^{\#3}$	90.0

Symmetry codes: #1) $-x$, $1-y$, z; #2) $-x$, y, $1-z$; #3) x, $1-y$, z.

Table S4. Selected bond lengths and angles for **1**·5C_2Cl_4·4CH_3OH at 123 K.

Fe1–N1	1.927(5)
Fe1–N2	1.998(3)
N1–Fe1–N2	90.000
N1–Fe1–N1$^{\#1}$	180.0
N1–Fe1–N2$^{\#1}$	90.000
N1–Fe1–N2$^{\#2}$	90.000
N1–Fe1–N2$^{\#3}$	90.000

Symmetry codes: #1) $-x$, $1-y$, z; #2) $-x$, y, $1-z$; #3) x, $1-y$, $1-z$.

6. Additional Figures

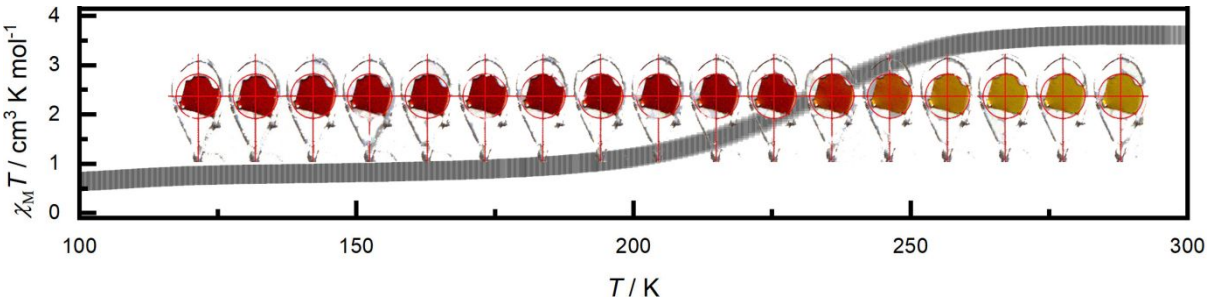

Figure S1. Temperature-dependent $\boldsymbol{\chi_M T}$ values and variable-temperature crystal colours of **1**·5C_2Cl_4·4CH_3OH.

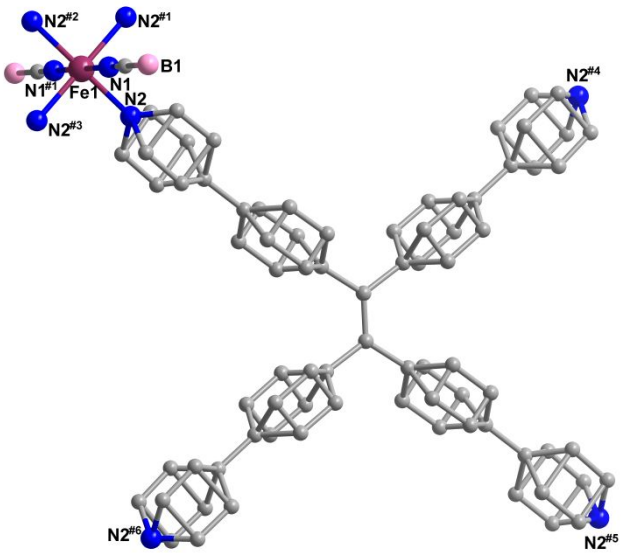

Figure S2. Coordination environment of the Fe^{II} atom in **1**·$5C_2Cl_4$·$4CH_3OH$ at 298 K and 123 K (Table S3, S4).

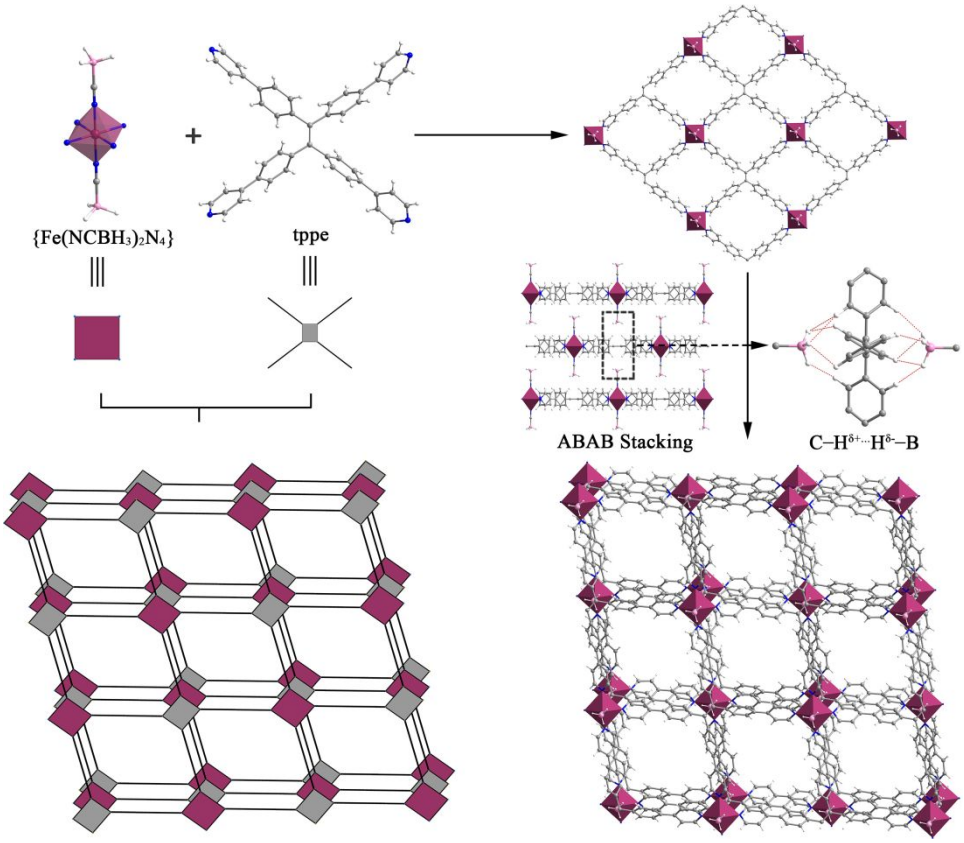

Figure S3. The supramolecular structure of **1**·$5C_2Cl_4$·$4CH_3OH$.

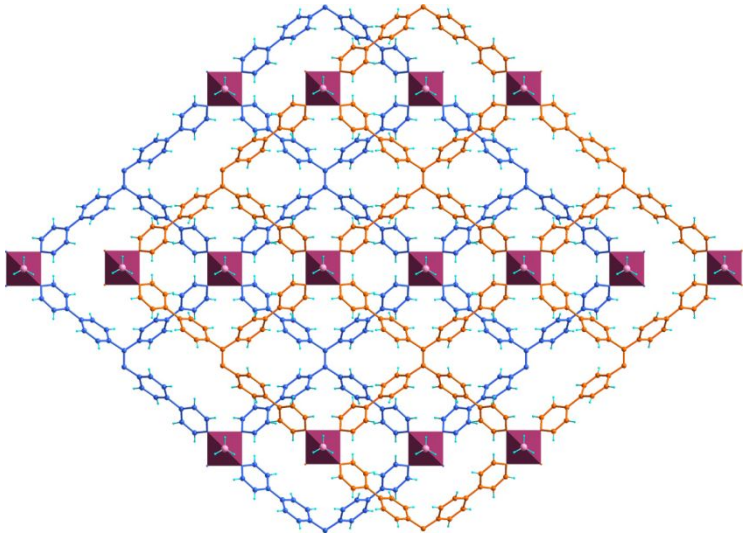

Figure S4. Another imaginary ABAB-stacked structure, in which the $\mathbf{NCBH_3^-}$ groups point to the windows of adjacent layers.

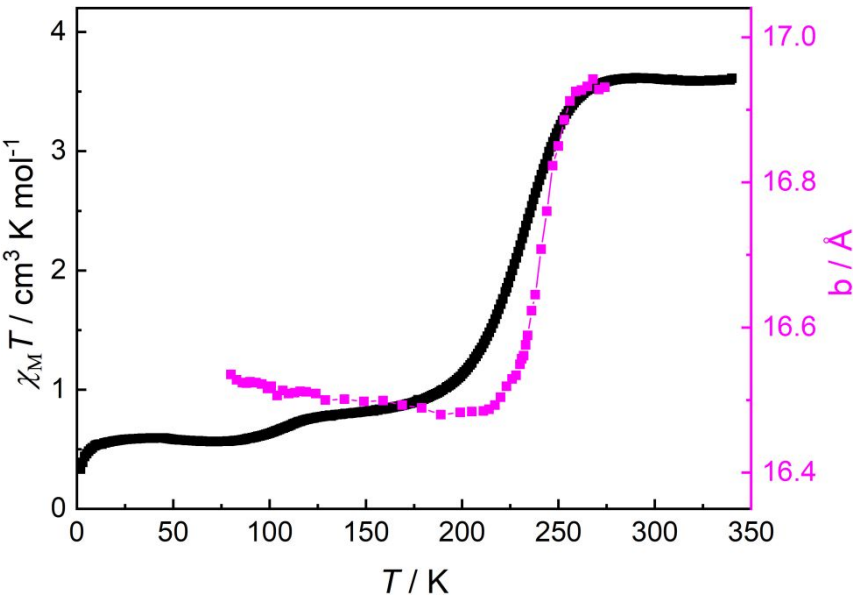

Figure S5. Temperature-dependent $\boldsymbol{\chi_M T}$ values and the variable-temperature *b*-axis values of **1**·5C_2Cl_4·4CH_3OH.

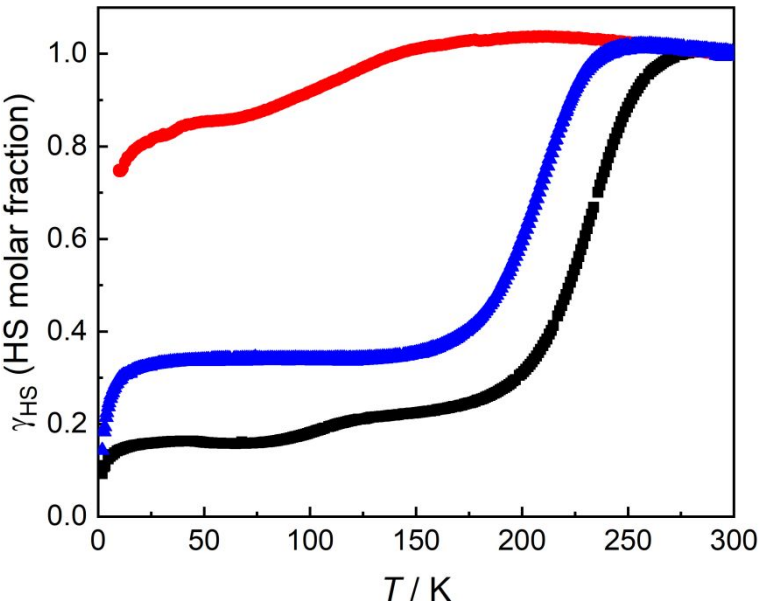

Figure S6. Temperature-dependent $\chi_M T$ values of **1**·5C_2Cl_4·4CH_3OH (black), **1**·3$CHCl_3$·4CH_3OH (blue), and **1**·2C_6H_6·4CH_3OH (red).

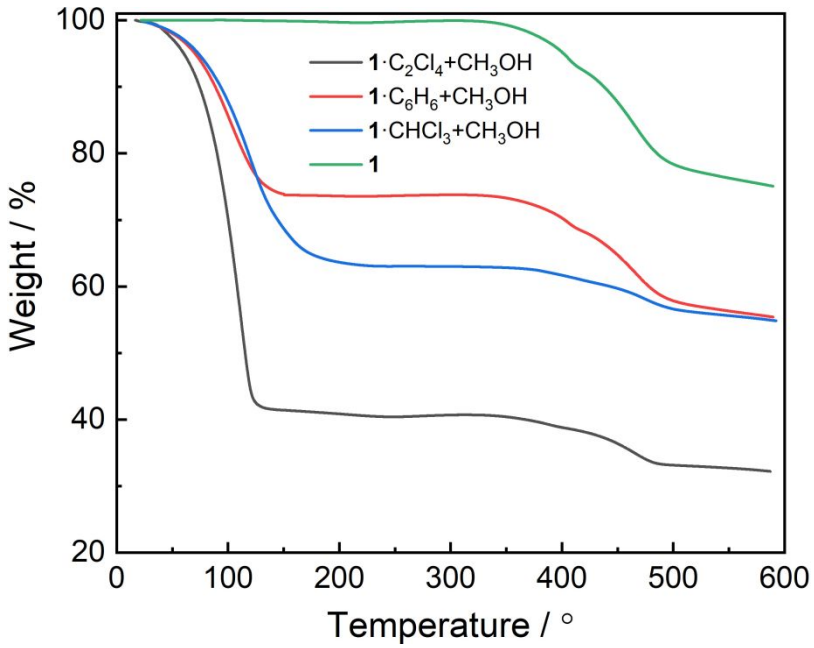

Figure S7. Thermogravimetric analysis of **1**·5C_2Cl_4·4CH_3OH, **1**·3$CHCl_3$·4CH_3OH, **1**·2C_6H_6·4CH_3OH, and **1**.

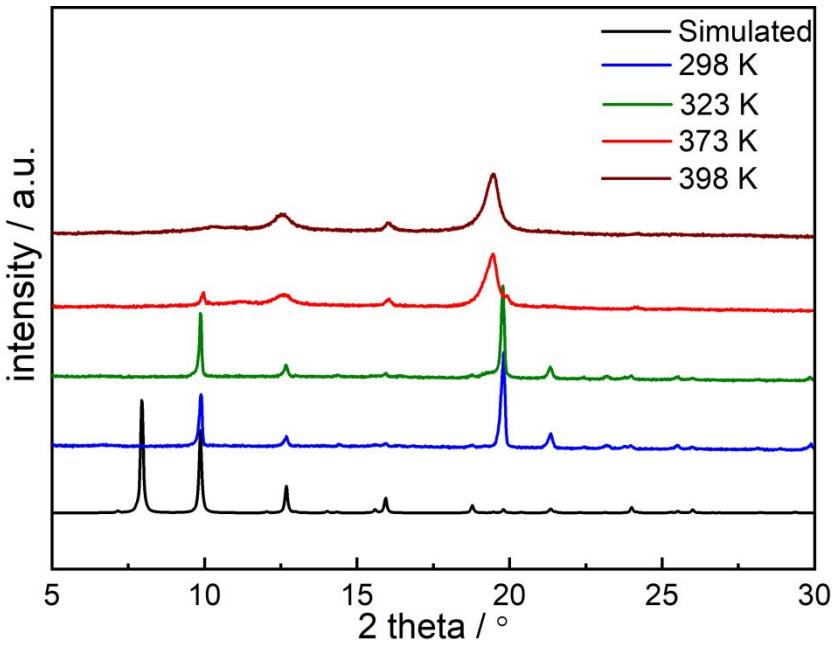

(a)

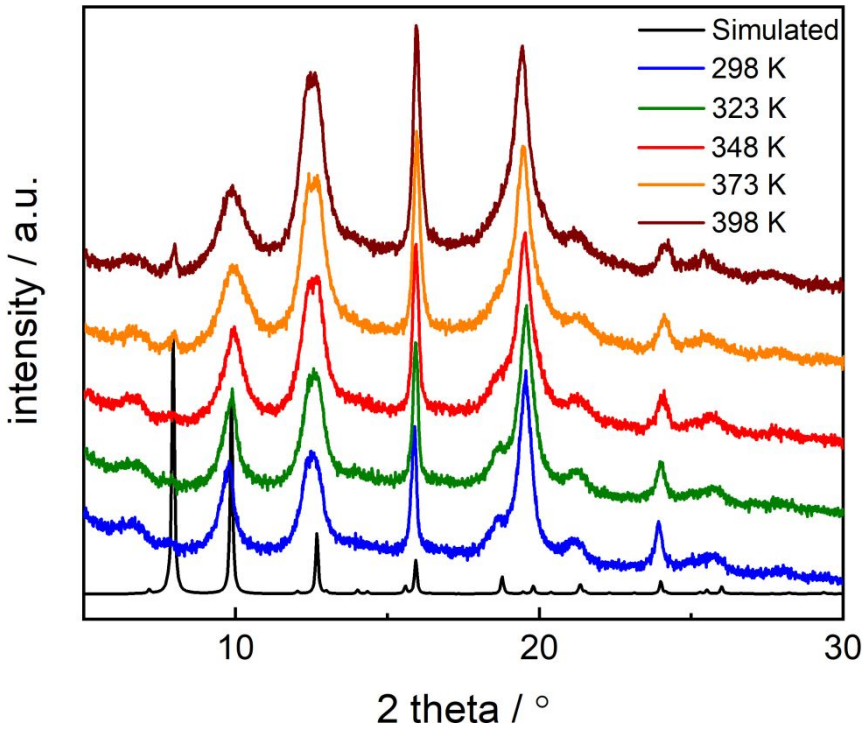

(b)

Figure S8. Variable-temperature powder X-ray diffraction pattern of compound **1**·$5C_2Cl_4$·$4CH_3OH$ in freshly prepared state (a) and stored for 6 months (b).

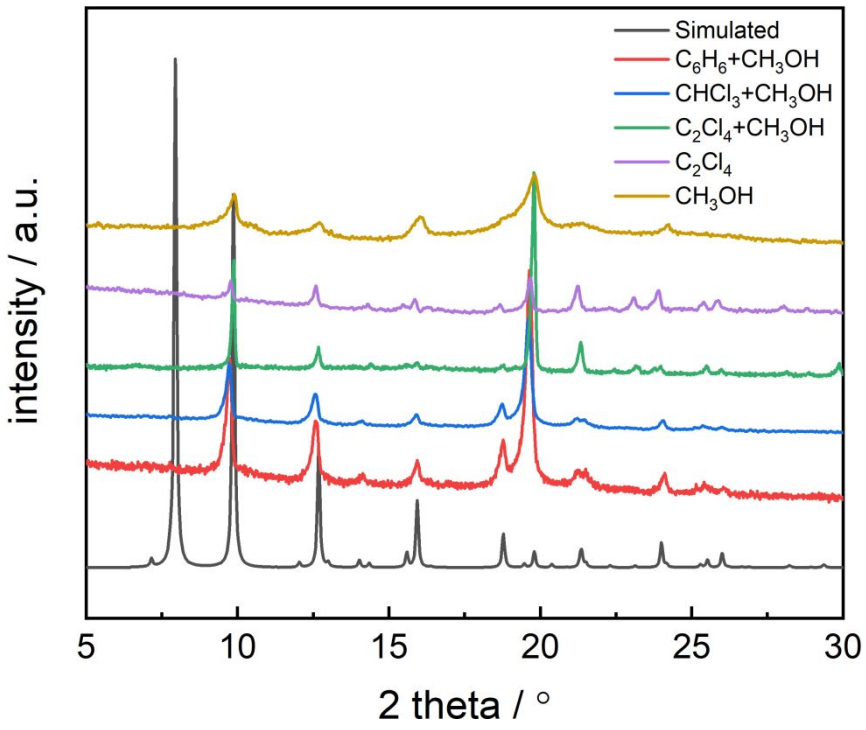

Figure S9. Powder X-ray diffraction pattern of compounds of **1**·$5C_2Cl_4$·$4CH_3OH$, **1**·$3CHCl_3$·$4CH_3OH$, **1**·$2C_6H_6$·$4CH_3OH$ and **1** encapsulating CH_3OH and C_2Cl_4 at 298 K.

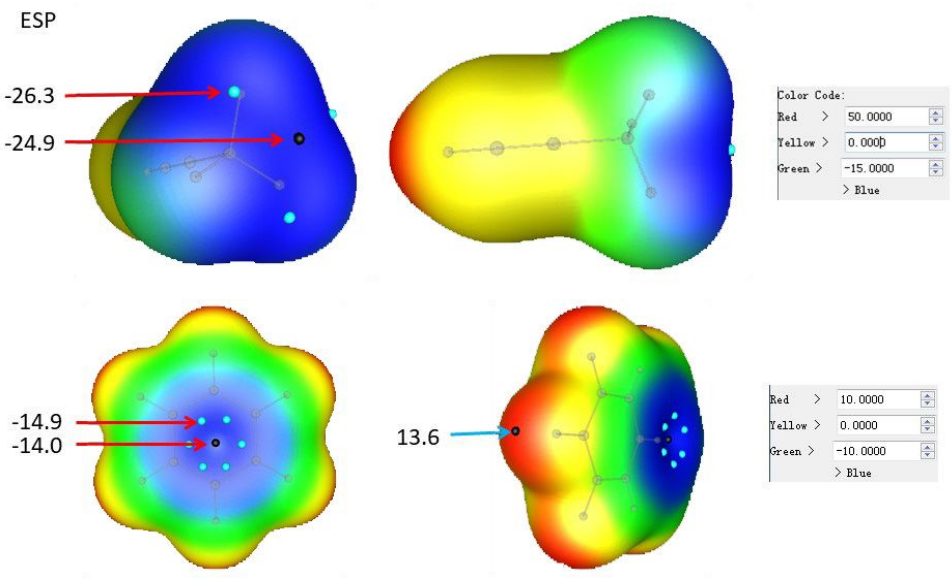

Figure S10. Electrostatic potential diagram and extreme value of $C_6H_6\cdots[NCBH_3^-]$ complex.

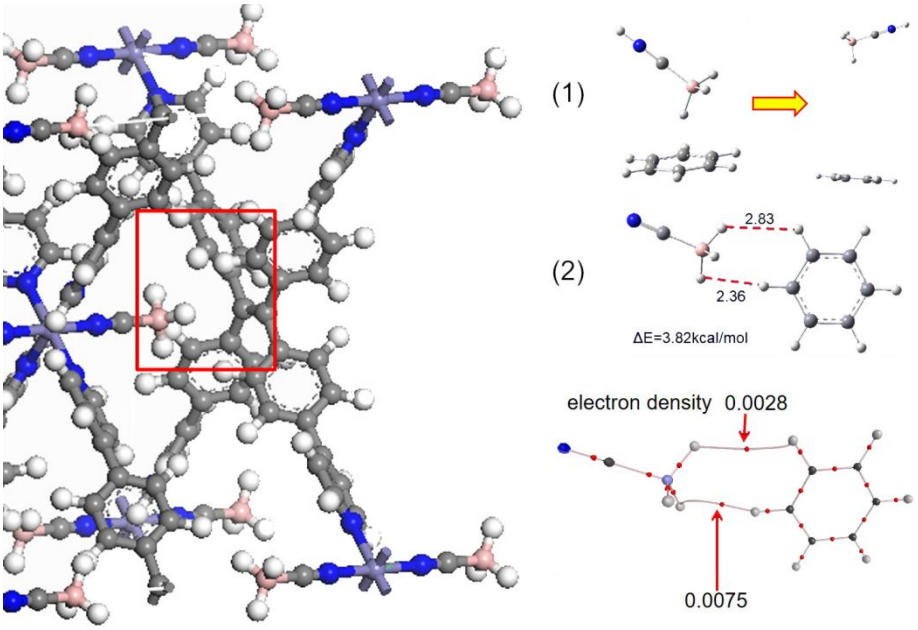

Figure S11. The dihydrogen bonds portion in the structure and electron density and molecular configuration of $C_6H_6\cdots[\mathbf{NCBH_3^-}]$ complex.

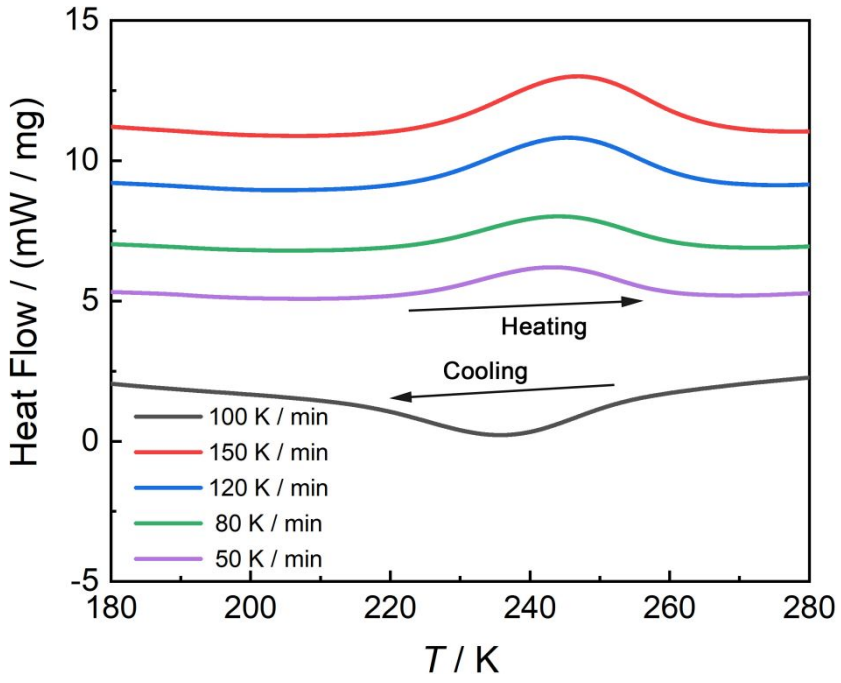

Figure S12. DSC data of compound **1**·$5C_2Cl_4$·$4CH_3OH$.

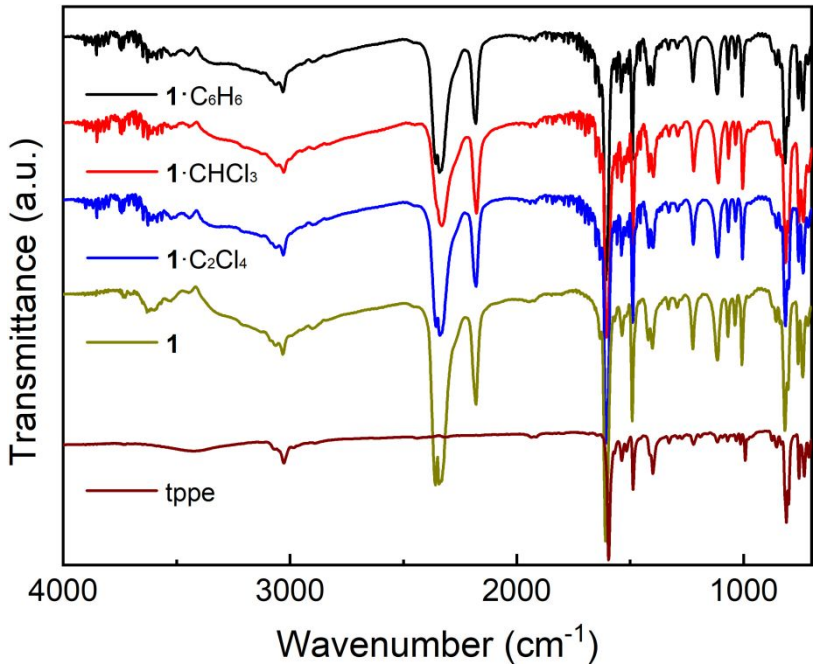

Figure S13. IR spectra of compounds **1**·$5C_2Cl_4$·$4CH_3OH$, **1**·$3CHCl_3$·$4CH_3OH$, **1**·$2C_6H_6$·$4CH_3OH$, **1** and tppe.

7. References

(1) (a) Altomare, A.; Burla, M. C.; Camalli, M.; Cascarano, G. L.; Giacovazzo, C.; Guagliardi, A.; Moliterni, A. G. G.; Polidori, G.; Spagna, R. *J. Appl. Crystallogr.* **1999**, *32*, b115; (b) Sheldrick, G. M.; *SHELXL-97*; Program for refinement of crystal structures. University of Göttingen, Göttingen, Germany, **1997**.

(2) (a) Spek, A. L. Utrecht University: Utrecht, The Netherlands, **1998**; (b) Spek, A. L. *Acta Cryst.* **2009**, *D65*, 148.

(3) (a) Taylor, R.; Macrae, C. F.; *Acta Cryst.* **2001**, *B57*, 815. (b) Bruno, I. J.; Cole, J. C.; Edgington, P. R.; Kessler, M. K.; Macrae, C. F.; McCabe, P.; Pearson J.; Taylor R. *Acta Cryst.* **2002**, *B58*, 389; (c) Macrae, C. F.; Edgington, P. R.; McCabe, P.; Pidcock, E.; Shields, G. P.; Taylor, R.; Towler, M.; van de Streek, J. *J. Appl. Cryst.* **2006**, *39*, 453; (d) Macrae, C. F.; Bruno, I. J.; Chisholm, J. A.; Edgington, P. R.; McCabe, P.; Pidcock, E.; Rodriguez-Monge, L.; Taylor, R.; van de Streek, J.; Wood, P. A. *J. Appl. Cryst.* **2008**, *41*, 466.

(4) (a) Stratmann, R. E.; Scuseria, G. E.; Frisch, M. J. *J. Chem. Phys.* **1998**, *109*, 8218; (b) Bauernschmitt, R.; Ahlrichs, R. *Chem. Phys. Lett.* **1996**, *256*, 454; (c) Casida, M. E.; Jamorski, C.; Casida, K. C.; Salahub, D. R. *J. Chem. Phys.* **1998**, *108*, 4439.

(5) Bernardi, F.; Boys, S. F. *Mol. Phys.* **1970**, *19*, 553.

(6) Frisch, M. J.; Trucks, G. W.; Schlegel, H. B.; Scuseria, G. E.; Robb, M. A.; Cheeseman, J. R.; Scalmani, G.; Barone, V.; Mennucci, B.; Petersson, G. A.; Nakatsuji, H.; Caricato, M.; Li, X.; Hratchian, H. P.; Izmaylov, A. F.; Bloino, J.; Zheng, G.; Sonnenberg, J. L.; Hada, M.; Ehara, M.; Toyota, K.; Fukuda, R.; Hasegawa, J.; Ishida, M.; Nakajima, T.; Honda, Y.; Kitao, O.; Nakai, H.; Vreven, T.; Montgomery, J. A.; Jr.; Peralta, J. E.; Ogliaro, F.; Bearpark, M.; Heyd, J. J.; Brothers, E.; Kudin, K. N.; Staroverov, V. N.; Keith, T.; Kobayashi, R.; Normand, J.; Raghavachari, K.; Rendell, A.; Burant, J. C.; Iyengar, S. S.; Tomasi, J.; Cossi, M.; Rega, N.; Millam, J. M.; Klene, M.; Knox, J. E.; Cross, J. B.; Bakken, V.; Adamo, C.; Jaramillo, J.; Gomperts, R.; Stratmann, R. E.; Yazyev, O.; Austin, A. J.; Cammi, R.; Pomelli, C.; Ochterski, J. W.; Martin, R. L.; Morokuma, K.; Zakrzewski, V. G.; Voth, G. A.; Salvador, P.; Dannenberg, J. J.; Dapprich, S.; Daniels, A. D.; Farkas, O.; Foresman, J. B.; Ortiz, J. V.; Cioslowski, J.; Fox, D. J. Gaussian 09 D.01. Gaussian, Inc.: Wallingford CT, **2013**.